
Mixing in vortical, chaotic and turbulent flows

J. C. Vassilicos

Phil. Trans. R. Soc. Lond. A 2002 **360**, 2819-2837

doi: 10.1098/rsta.2002.1093

Rapid response

[Respond to this article](#)

<http://rsta.royalsocietypublishing.org/letters/submit/roypta;360/1801/2819>

Email alerting service

Receive free email alerts when new articles cite this article - sign up in the box at the top right-hand corner of the article or click [here](#)

To subscribe to *Phil. Trans. R. Soc. Lond. A* go to:
<http://rsta.royalsocietypublishing.org/subscriptions>

Mixing in vortical, chaotic and turbulent flows

BY J. C. VASSILICOS

*Turbulence and Mixing Group, Department of Aeronautics,
Imperial College of Science, Technology and Medicine,
London SW7 2BY, UK*

Published online 24 October 2002

Mixing is discussed in relation to stirring as reflected in the geometry of advected interfaces, the behaviour of fluid-element pairs and their separation rates. Stirring is different in vortical, chaotic and turbulent flows because of qualitative differences in spatio-temporal flow structure, thus giving rise to different mixing laws. Important applications of the mixing and stirring properties discussed in this review are chlorine deactivation and ozone depletion in stratospheric mid-latitudes.

Keywords: vortex; ozone depletion; chaos; turbulence; mixing; fractals

1. Introduction

Fluid-mechanical mixing of scalar/tracer quantities such as chemicals, pollutants and heat occurs as a result of flow advection and molecular diffusion. Mixing occurs over scales ranging from kilometres in the Earth's mantle, the oceans and the atmospheres to metres and centimetres in combustion engines and chemical reactors and tens of micrometres in liquid-crystal flows. Topical cases where fluid-mechanical mixing is important are chlorine deactivation and ozone depletion in the stratosphere (McIntyre 1995; Pyle 1995).

In all these cases, advection stretches blobs or clouds of scalar quantities so that their bounding surface stretches and increases in area. This growth of surface area is usually accompanied by folding of the surface. Surface stretching carries on after folding, leading to repeated instances of stretching and folding of material surfaces. This is the stretch-and-fold mechanism extensively studied in the theory of low-dimensional nonlinear dynamical systems, but first mentioned in the context of turbulent pipe flow by Reynolds in his 1883 seminal experimental paper (see Monin & Yaglom 1975), which effectively launched the study of turbulent flows. More recently, the stretch-and-fold mechanism has also been studied in the context of stirring by chaotic (Ottino 1989) and vortical (Flohr & Vassilicos 1997) flows.

In the next section we describe the properties that distinguish vortical, chaotic and turbulent flows. All these flows generate increasingly small length-scales on the tracer field by leading to increasingly small separations between consecutive folds of stretched material surfaces. Mixing occurs when these length-scales are small enough for molecular diffusion to act perceptibly. However, qualitatively different flow fields generate increasingly small tracer scales in ways that are sufficiently different to lead to qualitatively different mixing laws. Mixing in vortical and chaotic flows is

One contribution of 20 to a Triennial Issue 'Astronomy and Earth science'.

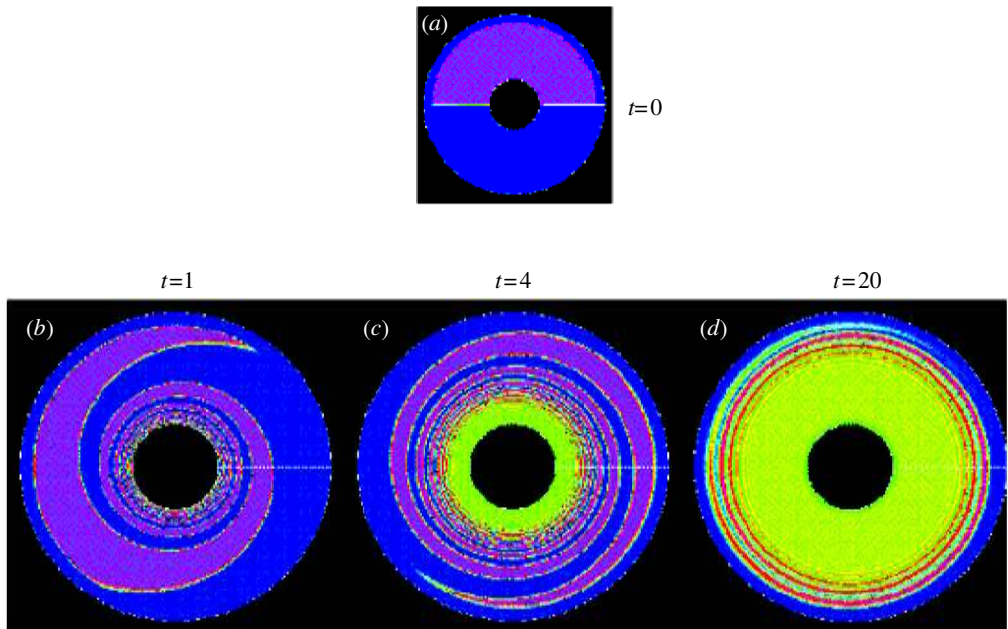


Figure 1. Scalar spiral structure in a vortex at different times. (a) Initial scalar concentration field. (b) Spiral interface curve starts to develop. (c) Spiral extends throughout the field and accelerated diffusion is observed near the centre. The outer gradients are still sharply defined. (d) The entire scalar field has mixed. (Reproduced from Flohr & Vassilicos (1997) with permission.)

discussed in §3 with an application to chlorine deactivation and ozone depletion over the mid-northern latitudes presented in §4. Stirring and mixing in turbulent flows is addressed in §5. All the flows we consider here are incompressible.

2. Vortical, chaotic and turbulent flows

Interfaces of scalar blobs are lines in two-dimensional flows and surfaces in three-dimensional flows. Most of the emphasis here is on two-dimensional flows both for simplicity of exposition and because three-dimensional flows remain less well understood.

(a) *Stretch and fold*

Two-dimensional steady vortex flows have streamlines surrounding their core and do not move. The local flow is a shear flow that causes fluid elements on different streamlines to separate linearly in time. Thus, the local shear across streamlines stretches material lines, while the vortical nature of these streamlines folds the material lines. What results is a spiral locally stretched by the local shear and folded around the vortex (see figure 1) with a length that grows linearly in time. This is the stretch-and-fold mechanism in two-dimensional steady vortices, and it is qualitatively different from the stretch-and-fold mechanism in chaotic flows that we describe next.

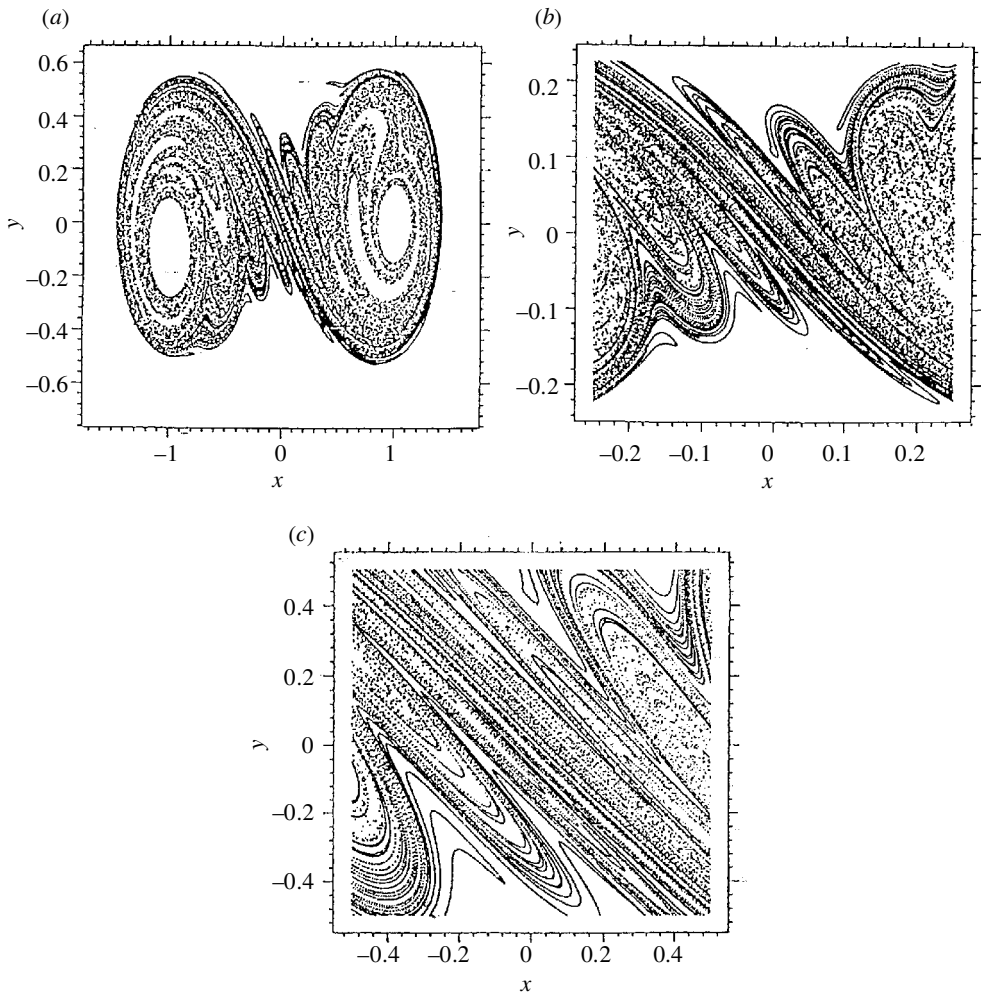


Figure 2. (a) Material line in a blinking vortex at time $t = 15T$. The central region is magnified in (b), and the central region of (b) is magnified in (c). (Reproduced from Fung & Vassilicos (1991) with permission.)

The flow acquires chaotic characteristics as soon as the vortex starts moving back and forth (Aref 1984; Ottino 1989). An extreme caricature of such a situation is the blinking vortex introduced by Aref (1984). The vortex jumps between two points at time-intervals T . Starting a material line between these two points, the vortex will first stretch and wind the line around itself into a fold or spiral for a period T , then jump to its other position from which it will stretch and wind the already folded or spiral line into a further fold or spiral, and so on repeatedly, eventually producing a stretched and folded structure that is qualitatively different from a simple spiral (see figure 2). This qualitative difference is felt in the rate of growth of the line, which is now exponential rather than linear (Ottino 1989).

A closer look, assisted by the theory of Hamiltonian dynamical systems (Lichtenberg & Lieberman 1983; Ottino 1989), reveals that the flow is not necessarily chaotic

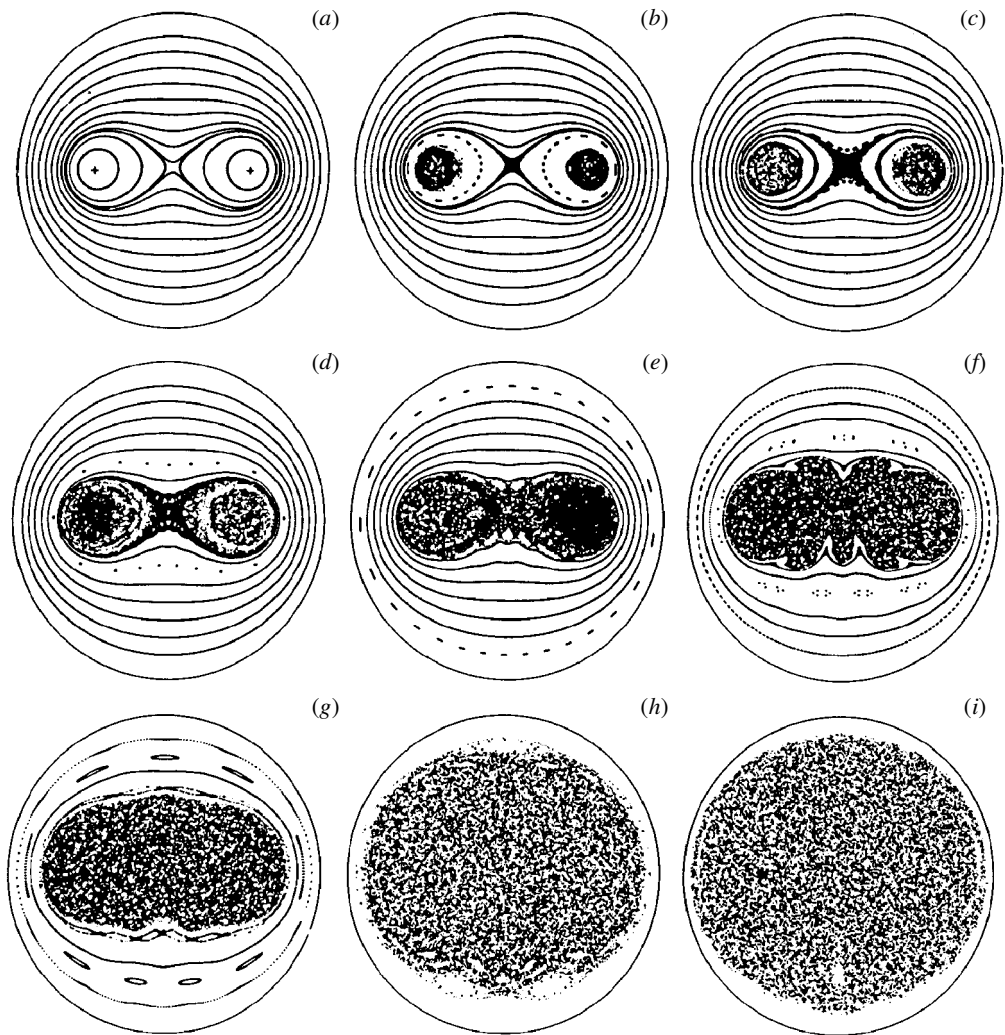


Figure 3. Poincaré sections corresponding to 15 initial conditions in the blinking vortex for different periods T non-dimensionalized against the circulation Γ of the vortex and the distance b between the two positions of the vortex. Poincaré sections record all the positions of a fluid element at time intervals equal to the period T . Values of $(\Gamma T)/(4\pi b^2)$: (a) 0.2; (b) 0.4; (c) 0.5; (d) 0.6; (e) 0.8; (f) 1.4; (g) 2.0; (h) 4.0; (i) 6.0. (Reproduced from Aref (1984) with permission.)

everywhere (i.e. globally chaotic). An important critical length is the radius of the instantaneous vortex streamline that has orbital time equal to T (Aref 1984; Wonhas & Vassilicos 2001). When the spatial extent of the vortex oscillations is small compared with that critical length (i.e. when T is large), the flow is fully chaotic inside a region of a size comparable with that of the critical length (Aref 1984). This means that fluid elements visit effectively every point inside that region (see figure 3) and material lines tend to eventually fill it completely. However, it must be noted that the time needed to fill that region can be very long and in the meantime material

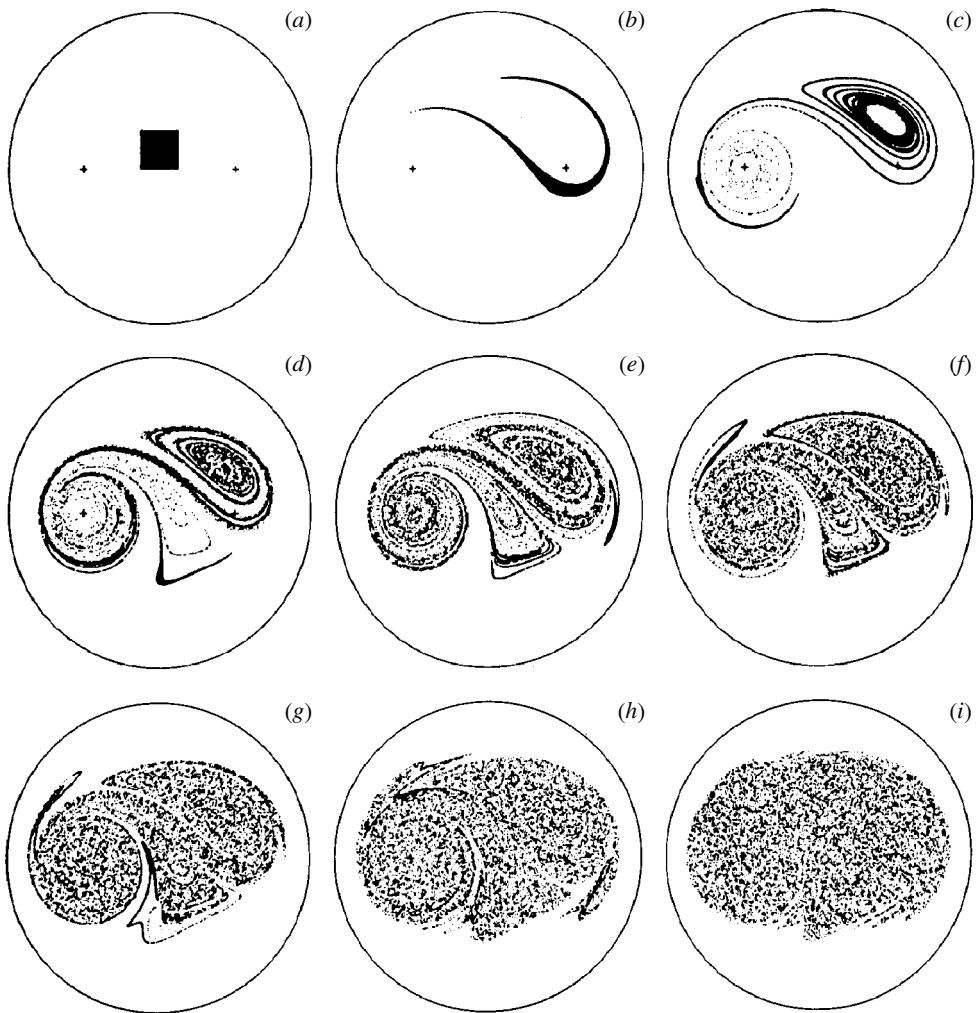


Figure 4. Different snapshots in the stirring by a blinking vortex of an initially square blob: (a) $t = 0$; (b) $t = T$; (c) $t = 2T$; (d) $t = 3T$; (e) $t = 4T$; (f) $t = 5T$; (g) $t = 6T$; (h) $t = 9T$; (i) $t = 12T$. (Reproduced from Aref (1984) with permission.)

lines can have very well defined spiral shapes before they develop the stretched and folded profile characteristic of chaotic advection (see figure 4). In the opposite limit, where T is very small, the flow tends towards the limiting situation where two steady co-rotating vortices generate a straining region (hyperbolic point) in between them (see figure 3), a circumstance which severely limits the extent of the chaotic regions, as shown in figure 3.

In the limit where T is large, and far away from the region where the vortex moves and where chaotic regions thrive, the motion of fluid elements is governed by a near-integrable Hamiltonian dynamical system (Wonhas & Vassilicos 2001), which means that a fluid element's velocity is that of the instantaneous vortex at the fluid element's position (which, by itself is integrable) plus a small correction due to the

periodic vortex motion (which makes the perturbed integral system non-integrable). The Poincaré–Birkhoff and Kolmogorov–Arnold–Moser (KAM) theorems (Lichtenberg & Leiberman 1983; Ottino 1989) describe how non-integrable periodic perturbations modify the properties of integrable Hamiltonian systems and can therefore be applied far enough away from the chaotic region of the blinking vortex. We refer to the references cited above for detailed accounts of these theorems. Here we only need to say that all vortex streamlines with orbital times incommensurate with T (i.e. integer multiples of the orbital time are not equal to integer multiples of T) give rise to closed periodic fluid-element trajectories around the vortex. These trajectories are slightly distorted versions of the vortex streamlines. They correspond to the celebrated KAM tori and constitute barriers to transport because any fluid element in them remains in them ad infinitum. However, they break-up as the perturbation is increased. Vortex streamlines with orbital times commensurate with T give rise to chaotic regions very thinly squeezed between KAM trajectories that they cannot penetrate. Wonhas & Vassilicos (2001) conclude that the advection in these outer regions is therefore dominated by KAM trajectories and that, at scales not too small to resolve the exceedingly thin chaotic regions, it resembles the flow of a steady vortex.

When the motion of the vortex is not periodic, as is the case of the stratospheric polar vortex (e.g. McIntyre 1995), KAM trajectories do not exist and the flow develops chaotic behaviour everywhere, as it does in other non-periodic shear flows (see those of Pierrehumbert (1994) and Antonsen *et al.* (1996)). Indeed, the Poincaré–Birkhoff and KAM theorems are not valid and do not have equivalents for non-periodic time-dependent flows (Ottino 1989; Pierrehumbert 1994). However, it must be stressed again, as in the case of the blinking vortex with large periodicity T (figure 4), that the time needed for this chaotic behaviour to fully manifest itself everywhere can be long. Wonhas (2001) has demonstrated that, when the diffusivity of the random motion is small compared with the circulation of the vortex, material lines in a randomly moving planar vortex develop a well-defined spiral structure away from the region where the vortex moves and a more chaotic stretched and folded structure closer to that region. More importantly, Wonhas (2001) has shown that the size of this inner chaotic region grows slowly, in fact only diffusively (as the square root of time for a classical point vortex), which means that a lot of the flow feels the action of the vortex but not that of the chaotic advection for a significantly long time. Of course, there are other non-periodic, time-dependent flows, such as the time-dependent, random shear flows of Pierrehumbert (1994), which manifest their globally chaotic advection quickly everywhere.

(b) *Pair separation*

Incompressible two-dimensional flows are such that, at any point and any time, there is a direction along which velocity gradients cause pairs of fluid elements to separate faster than in any other direction, and another direction along which particle pairs either contract (as in steady straining flows) or simply do not separate nor contract at all (as in steady shearing flows). (This well-known statement has its counterpart in incompressible three-dimensional flows.) We denote the locally fastest growing separation by $\Delta_+(\mathbf{x}, t)$ and note that it potentially has different growth rates for different initial positions \mathbf{x} . In steady vortex flows $\Delta_+ \sim t$. However, there must be at least some points \mathbf{x} in chaotic flows from which $\Delta_+ \sim e^{ht}$

with $h > 0$; otherwise interfaces would not grow exponentially as they indeed do in such flows. The exponents $h(\mathbf{x}, t)$ are called finite-time Lyapunov exponents when they are calculated at finite times and therefore vary with \mathbf{x} and t (Antonsen *et al.* 1996). For asymptotically large times t , the exponents $h(\mathbf{x}, t)$ tend to well-defined time-independent values h (Oseledec 1968; Eckmann & Ruelle 1985), and in regions of global chaos where fluid elements eventually visit the entire region, the exponents h are positive and the same for all initial positions \mathbf{x} in that region (Ottino 1989; Toussaint *et al.* 1995). In this case, h is called a Lyapunov exponent. However, the time, T_{conv} , needed for $h(\mathbf{x}, t)$ to start departing significantly from the neighbourhood of zero can be long (Eckhardt & Yao 1993; Toussaint *et al.* 1995), and the time needed to converge to the Lyapunov exponent h can be even longer and comparable with the time that fluid-element trajectories take to fill the globally chaotic region (figures 3 and 4 give an indication of how long it can take to fill that region). In fact, a glance at figures 3 and 4 suggests that for times $t \ll T_{\text{conv}}$ the time-dependence of Δ_+ may not be exponential at all in many parts of the flow but perhaps even just linear where, and as long as, the transient spiral interfacial structures are developing. Where chaotic and regular regions coexist, $h(\mathbf{x}, t)$ tends to zero for sufficiently long times in those regions that are regular and where we may therefore expect $\Delta_+ \sim t$, and towards different positive Lyapunov exponents in different chaotic regions (e.g. Toussaint *et al.* 1995).

(c) Fractal geometry

The stretch-and-fold mechanisms and the increasing length of material lines inside finite regions of vortical and chaotic flows imply that a broad distribution of length-scales develops on these lines. A measure of this distribution is the box-counting function $N(\delta, t)$, which is a central quantity of fractal geometry. Given a grid of resolution (grid-cell size) δ covering the two-dimensional space of the flow, the number of cells containing a part of the material line at time t is $N(\delta, t)$. This number is larger for finer resolutions, i.e. for smaller δ . The rate with which this number increases with increasing resolution gives an indication of the amount of space that is filled by the line. Straight or otherwise regular lines are such that $N(\delta) \sim \delta^{-1}$. However, for material lines in fully chaotic flow regions, $N(\delta, t)$ tends to a δ^{-2} scaling as time advances and reaches that limit for times at least larger than T_{conv} (Toussaint & Carrière 1999; Ott & Antonsen 1989). This δ^{-2} scaling reflects the space-filling nature of lines in globally chaotic flow regions after long times, as can indeed be witnessed from figures 2 and 4. At transient times smaller than T_{conv} , the scaling of $N(\delta, t)$ is well approximated by $\delta^{-D(t)}$, where $D(t)$ takes values between 1 and 2 and in fact increases with time towards 2 (Fung & Vassilicos 1991). At the other extreme, lines in steady vortices develop a spiral structure with scaling $N(\delta) \sim \delta^{-D}$, where D can take values between 1 and 2 (Flohr & Vassilicos 1997). The exponent D is called the fractal or box-counting dimension or Kolmogorov capacity and is well-defined for many fractal and spiral geometries (Vassilicos & Hunt 1991). Where chaotic and regular regions coexist, parts of the line become chaotically space filling, while others remain regular or develop spiral structures, and the form of $N(\delta)$ must be considered to result from a potentially intricate combination of these effects.

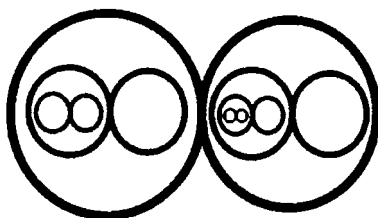


Figure 5. Schematic of the self-similar streamline topology consisting of cat eyes within cat eyes.

(d) *Turbulence*

Instantaneous snapshots of the velocity field of a vortex or chaotic flow are smooth and consist of one or a few vortices or other shearing motions of a given size. In contrast, instantaneous snapshots of turbulent flows are irregular and are made of an entire hierarchy of eddies over a wide range of length-scales. This hierarchy of eddies is most commonly described in terms of the energy spectrum $E(k)$ of the turbulence that measures the amount of energy in velocity fluctuations of wavenumber, k . Spatially homogeneous non-decaying turbulence is characterized by Kolmogorov's celebrated $k^{-5/3}$ form of $E(k)$ over a wide range of wavenumbers (Monin & Yaglom 1975). A statistically homogeneous and non-decaying turbulent flow with such a spectrum in two dimensions has been created in the laboratory by Paret & Tabeling (1997), using electromagnetically driven thin, stably stratified layers of NaCl solution. Fung & Vassilicos (1998) numerically simulated such a two-dimensional statistically homogeneous and non-decaying turbulence with a $k^{-5/3}$ energy spectrum by randomly adding incompressible Fourier modes with the appropriate amplitudes. They found that instantaneous snapshots of the turbulent velocity (in fact streamline) field have a self-similar topology made of cat eyes within cat eyes (figure 5). A pair of cat eyes is a streamline structure consisting of two co-rotating vortices and one straining hyperbolic point in between (see figure 3a). The spatial irregularity of the turbulent velocity field is therefore underpinned by this self-similar topology. Smaller cat eyes have smaller time-scales determined by $E(k)$ and are therefore essential in turbulent mixing.

For progressively smaller viscosities of the fluid, the self-similar topological structure of the turbulence acquires progressively more and smaller cat eyes more closely packed against each other, and the velocity field therefore tends towards a spatially singular velocity field with infinitesimally small spatial oscillations between infinitesimally close stagnation points. This singular limit is not a peculiarity of the particular turbulent flow discussed here (Paret & Tabeling 1997; Fung & Vassilicos 1998), but of any turbulent flow with a $k^{-5/3}$ energy spectrum, though it may well be that other types of singular topologies arise in other turbulent flows with such a spectrum.

The point has been made recently (Falkovich *et al.* 2001) that fluid-element pairs initially infinitesimally close to each other in a spatially singular velocity field separate neither linearly nor exponentially in time; and indeed Richardson's law (see Monin & Yaglom 1975) stipulates that in non-decaying homogeneous turbulent flows with a $k^{-5/3}$ energy spectrum, $\langle |\Delta|^2 \rangle \propto t^3$, where $\Delta = \Delta(\mathbf{x}, t)$ is the vector linking a pair of fluid elements together and the brackets signify an average over many such

fluid-element pairs over all space. Jullien *et al.* (1999) have confirmed Richardson's law in the turbulent flow of Paret & Tabeling (1997), and so have Fung & Vassilicos (1998) in their numerical model of that flow.

3. Mixing in vortical and chaotic flows

The process of stirring the passively advected concentration field $c(\mathbf{x}, t)$ is described mathematically by $(D/Dt)c = 0$ (Ottino 1989; Batchelor 1969), where D/Dt is the time derivative following a fluid element in its motion ($D/Dt = \partial/\partial t + \mathbf{u} \cdot \nabla$ for a velocity field $\mathbf{u}(\mathbf{x}, t)$). Stirring is perhaps more intuitive in terms of the vector Δ linking a *pair* of fluid elements that evolves through the action of velocity gradients across Δ , i.e. $D\Delta/Dt = \Delta \cdot \nabla \mathbf{u}$ (Batchelor 1969).

It is because stirring causes fluid-element pairs to separate and therefore other pairs to come close together by incompressibility that concentration gradients ∇c increase in time, thus reflecting the production of increasingly small scales in the concentration field. This is expressed mathematically by the conservation law

$$\frac{D}{Dt}(\Delta \cdot \nabla c) = 0, \quad (3.1)$$

which is an algebraic consequence of the two previous equations. Hence, in the direction of fastest pair separation (Δ_+) the concentration gradients decrease, but they increase in the directions in which pairs tend to converge towards each other. This means that isoconcentration surfaces (or lines in two dimensions) tend to align themselves with the fastest growing pair separation and high concentration gradients build up in the perpendicular direction. The rates of fastest and slowest pair-separation growths determine each other by incompressibility, and they also determine the generation of concentration gradients and therefore of small scales on the concentration field. Knowledge of $\Delta_+(\mathbf{x}, t)$ therefore provides a complete description of stirring. How much can $\Delta_+(\mathbf{x}, t)$ tell us about mixing?

Mixing results from the interaction between stirring and molecular diffusion and is described mathematically by

$$\frac{D}{Dt}c = \kappa \nabla^2 c, \quad (3.2)$$

where κ is the molecular diffusivity of the concentration scalar c . The spatially averaged concentration $\langle c \rangle \propto \int d\mathbf{x} c(\mathbf{x}, t)$ remains constant in time and a measure of mixing must therefore be the variance $c'^2 \equiv \langle (c - \langle c \rangle)^2 \rangle$, which, in the presence of molecular diffusion, is a decreasing function of time until it reaches zero, when $c = \langle c \rangle$ everywhere in the flow and the scalar concentration c is well mixed.

As originally argued by Durbin (1980), mixing occurs when fluid elements are brought together by stirring, and the scalar concentrations that they carry diffuse molecularly into each other. Durbin (1980) further argued (but see also Falkovich *et al.* 2001) that mixing measured by the variance c'^2 can be calculated from the statistics of fluid-element pairs, and therefore from knowledge concerning $\Delta_+(\mathbf{x}, t)$. In the general context of Durbin's (1980) approach, a formula has been derived (Antonsen *et al.* 1996; Wonhas & Vassilicos 2002a) for mixing in *non-turbulent* flows that encapsulates different mixing behaviours and mechanisms in different types of flow. This formula relates $c'^2(t)$ to $\Delta_+(\mathbf{x}, t)$ and to the initial concentration field

$c_0(\mathbf{x}) = c(\mathbf{x}, 0)$ when no source of scalar fluctuations is used to replenish the variance lost through mixing (no scalar forcing),

$$c'^2(t) \propto \int d\mathbf{x} (c_0(\mathbf{x}) - \langle c_0 \rangle)^2 \times \exp \left[-2\kappa a_0^{-2} s^2(\phi) \int_0^t d\tau \Delta_+^2(\mathbf{x}, \tau) \right], \quad (3.3)$$

where a_0 is some conserved characteristic area (in incompressible two-dimensional flow), ϕ is the local initial angle between the local scalar gradient and the local direction of fastest pair separation and $s(\phi)$ is either equal to $\sin \phi$ in steady straining or chaotic flows or is a constant independent of ϕ in steady shearing or vortical flows without chaos.

We mention this apparently complicated formula for two reasons. The first reason is conceptual: this formula directly relates the decay of the scalar variance, which is a measure of mixing, to the growth of pair separations, which is a measure of stirring. The second reason, which we detail in the rest of this section, is that it leads to correct mixing rates (decay of $c'^2(t)$ in time) in flows as different as globally chaotic on the one hand and steady vortical on the other.

In the case of those globally chaotic flows where fluid-element pairs quickly adopt exponential separation rates everywhere in the flow (such as the flows of Pierrehumbert (1994) and Antonsen *et al.* (1996), and the Baker map of Wonhas & Vassilicos (2002a)), $\Delta_+(\mathbf{x}, t) \sim e^{ht}$ with $h(\mathbf{x}, t) > 0$ and equation (3.3) successfully predicts superexponential decay of the scalar variance $c'^2(t)$ for early times (Pierrehumbert 1994; Antonsen *et al.* 1996; Wonhas & Vassilicos 2002a). During this initial decay period, more than 90% (in the flows considered in the references just mentioned) of the scalar variance is lost, and the mixing mechanism behind this loss is rooted in the exponential separation of fluid-element pairs.

The decay of the rest of the variance for longer times turns out to be exponential (Pierrehumbert 1994; Antonsen *et al.* 1996). Antonsen *et al.* (1996) have argued that the dominant long time contribution to the decay of scalar variance comes from scalar gradients oriented close to the direction of fastest pair separation ($\phi = 0, \pi$) because these gradients are the last to survive molecular diffusion (see comments under equation (3.1)). The long-term decay is therefore dominated by those exponential terms in equation (3.3) with $s(\phi) = 0$ which survive superexponential decay, and a further calculation based on equation (3.3) reveals that these surviving terms decay only exponentially (Antonsen *et al.* 1996).

This long-term mixing mechanism based on long-term surviving scalar gradients aligned in the direction of fastest pair separation is, however, not the only mechanism that can lead to long-term exponential decay. Fereday *et al.* (2002) and Wonhas & Vassilicos (2002a) have identified a different mechanism that is not incorporated in equation (3.3), which also leads to long-term exponential decay and which is based on how the spatial non-uniformity of velocity gradients affects the global structure and spatial variations of the entire scalar field. This global mechanism is not captured by equation (3.3), which locally integrates pair trajectories, nor in any other local trajectory theory predicting exponential scalar variance decay. The range of validity of equation (3.3) and the circumstances when one or the other exponential decay mechanism prevails are unknown and the object of current research. However, quite surprisingly perhaps, equation (3.3) holds in it one more mixing mechanism, the fractal/spiral decay mechanism.

In the case of steady vortical flows, as in the case of any steady shear flow, pair separations grow linearly, i.e. $\Delta_+ \sim t$, and the argument in the exponential in equation (3.3) is proportional to t^3 rather than to an exponential function of time. The rate of scalar variance decay is therefore much slower in a steady vortex than it is in globally chaotic advection, but this does not mean that the action of the vortex does not accelerate scalar mixing. The mechanism whereby the vortex does accelerate scalar mixing is based on the spiral gradient structure imposed on the scalar field by the two-dimensional vortex (see figure 1). It is striking how, in figure 1, the scalar concentration appears fairly well mixed near the centre of the vortex at a time when the gradients at the outer arms of the scalar spiral remain sharp! This is the mark of the fractal/spiral mixing mechanism. The spiral gradient structure introduces an increased spatial decorrelation of the scalar concentration field, increased by comparison with the spatial decorrelation due to a single isolated sharp scalar gradient. It is this spatial decorrelation that lies behind the well-known fact that sharp gradients decay quickly. Increasing this spatial decorrelation by stretching and folding the line of high scalar gradients, and thereby creating a decorrelating accumulation of gradients, increases the decay rate and mixing of the scalar field (Angilella & Vassilicos 1998) even further. In the case of the steady vortex, this gradient accumulation occurs in a spiral way (figure 1).

This mechanism can also be derived from equation (3.3) in the case of the steady vortex where $\Delta_+ \sim t$. Carrying out the spatial integration in equation (3.3) leads to (Flohr & Vassilicos 1997; Wonhas & Vassilicos 2001, 2002a)

$$c'^2(0) - c'^2(t) \propto \left(\frac{\eta(t)}{L} \right)^{2-D} \quad (3.4)$$

for $\eta(t)/L \ll 1$, where L is a length-scale characterizing the initial concentration patch, D is the fractal dimension of the spiral gradient structure imposed on the scalar field by the two-dimensional vortex ($1 \leq D < 2$) and $\eta(t) \sim \kappa^{1/2} t^{3/2}$ is the diffusive microscale at time t . The mixing law (3.4) has been computationally verified in both steady and weakly unsteady two-dimensional vortices (Flohr & Vassilicos 1997; Wonhas & Vassilicos 2001).

The mixing law (3.4) is a reflection of the fractal/spiral mixing mechanism described above because the fractal dimension D is a measure of the spatial decorrelation of the scalar concentration field. The larger the value of D , the more space-filling the line of sharp scalar gradients and therefore the higher the spatial decorrelation of the scalar field leading to faster algebraic mixing. Mixing law (3.4) is in fact valid quite broadly, including for the decay of fractal structures without fluid flow, in which case $\eta(t) \sim \sqrt{\kappa t}$ (see Angilella & Vassilicos 1998). Wonhas & Vassilicos (2002b) argue that (3.4) is valid whenever the fractal dimension D of the line of scalar concentration gradients is strictly less than 2, which is not the case in globally chaotic flows with small T_{conv} everywhere. By the way, in the case of such globally chaotic flows with superexponential followed by exponential mixing, the mixing rate $(d/dt)c'^2(t)$ is independent of diffusivity or, at the very least, only logarithmically dependent (Pierrehumbert 1994; Wonhas & Vassilicos 2002a). This contrasts with the diffusivity dependence of $(d/dt)c'^2(t)$ caused by the fractal/spiral mixing mechanism, in which case such a dependence exists and is algebraic (from equation (3.4), $\sim \kappa^{1-D/2}$). This qualitative difference in diffusivity dependencies plays an important role in the following section.

4. Chlorine deactivation and ozone depletion in the stratosphere

In a cold arctic winter, polar stratospheric clouds form and heterogeneous chemical reactions in these clouds produce chlorine monoxide radicals (Peter 1994). This chlorine-activated air can subsequently be transported by stratospheric winds to mid-northern latitudes (Pyle 1995), where it can catalytically deplete ozone with the result of increasing ultraviolet radiation over densely populated areas. However, chlorine monoxide may itself be deactivated before it has had the time to destroy ozone. One such deactivation mechanism involves the reaction between polar air (rich in chlorine monoxide) and mid-latitude air (rich in nitrogen oxides) (Chipperfield *et al.* 1997). For this reaction to occur, fluid elements of polar and mid-latitude air need to be brought into close proximity by stratospheric stirring and then diffuse into each other.

Owing to the stable stratification of the stratosphere, stirring by stratospheric winds is two dimensional and therefore we might expect that our current understanding of two-dimensional stirring and mixing might be applicable. Tan *et al.* (1998) used such winds measured by the European Centre for Medium-range Weather Forecasts (ECMWF) to simulate on the computer the mixing and subsequent chemical reaction of chlorine monoxides, ClO, originating from polar regions with nitrogen oxides NO_x in the mid-latitudes. These reactions deactivate chlorine monoxides by producing chlorine nitrates, e.g. $\text{ClO} + \text{NO}_2 \rightarrow \text{ClONO}_2$.

The longitudinal and latitudinal resolution of the ECMWF wind measurements is *ca.* 4°, the time resolution *ca.* 6 h and the customary assumption is made that the velocity field below this resolution acts as a turbulent diffusivity κ_t on the chemicals. Hence, Tan *et al.* (1998) integrated the following coupled equations ($i = 1, 2$), which incorporate advection and diffusion as in (3.2), but also a chemical reaction,

$$\frac{D}{Dt}c_i = \kappa_t \nabla^2 c_i - \gamma c_1 c_2, \quad (4.1)$$

$$\frac{D}{Dt}c_3 = \kappa_t \nabla^2 c_3 + \gamma c_1 c_2, \quad (4.2)$$

where c_1 , c_2 and c_3 are the concentration fields of ClO, NO₂ and ClONO₂ respectively; γ is the chemical reaction constant and $D/Dt = (\partial/\partial t) + \mathbf{u} \cdot \nabla$, where \mathbf{u} is the ECMWF stratospheric velocity wind field.

Tan *et al.* (1998) solved these equations on the computer using a stratospheric incompressible velocity field interpolated on the 475 K isentrope (an altitude of *ca.* 20 km). They calculated the total amount of chlorine nitrate, ClONO₂, produced throughout the flow on different days and for different turbulent diffusivities κ_t . They found that the total amount of ClONO₂ produced has a power-law dependence on diffusivity and that this power law is different on different days.

Solving on the computer for the advection of chlorine monoxide ($i = 1$) originating from polar regions (i.e. solving (4.1) with ECMWF winds but without the diffusion and the chemical reaction terms) leads to a stretched and folded concentration field exhibiting both spiral and chaotic features (figure 6). The mixing, and therefore the chemical reaction, between polar chlorine monoxide and mid-latitude nitrogen oxides occurs across this stretched and folded interface in figure 6. Wonhas & Vassilicos (2002*b*) noted that the chemical reactions in the calculation of Tan *et al.* (1998) are so fast that they are effectively limited by the advection–diffusion process rather

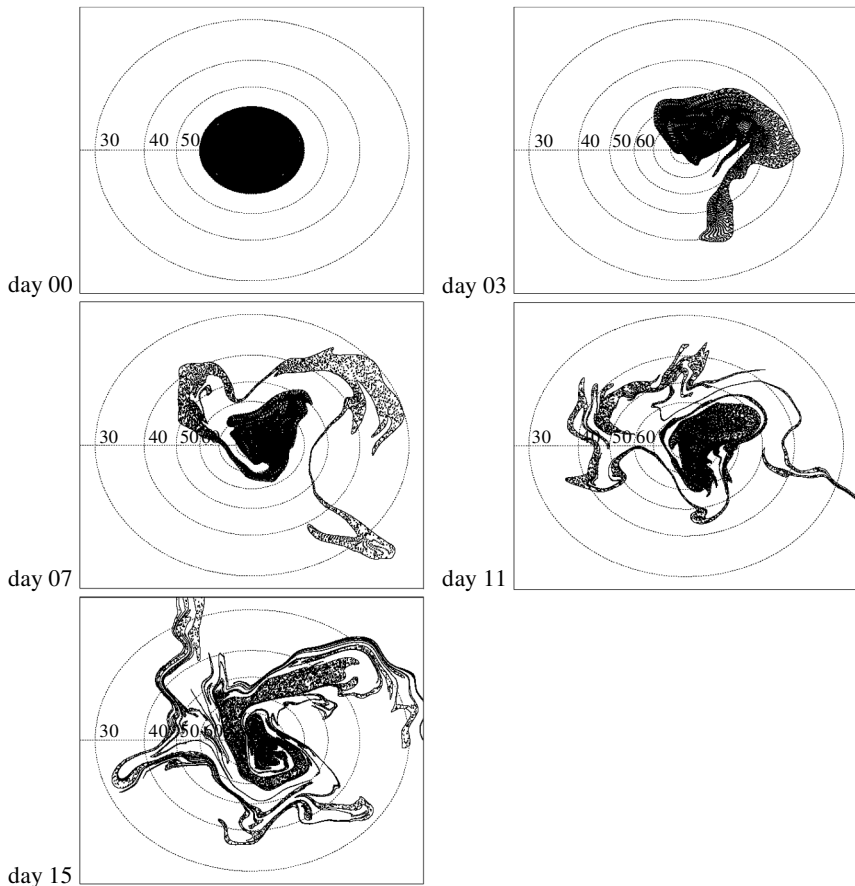


Figure 6. Stereographic projections of an interface on different days. Latitudes are depicted by dotted lines in 10° intervals with latitudes 30° N to 60° N indicated by numerals 30–60. On the first day of the simulation, 9 January 1992, the interface is aligned with the 60° N latitude. (Reproduced from Wonhas (2001) with permission.)

than by the reaction speed. As a consequence, for small enough diffusivity κ_t , and for initial conditions such as those of figure 6 and Tan *et al.* (1998), the total amount of ClONO₂ produced is proportional to the variance of $c_1 - c_2$. The progress variable $c_1 - c_2$ is governed by advection and diffusion alone, i.e. an equation such as (3.2). Hence, the power-law dependence of the total amount of ClONO₂ on diffusivity κ_t might suggest a fractal/spiral mixing mechanism quantified by a relation such as (3.4) rather than chaotic mixing.

To test this suggestion, Wonhas (2001) integrated pair separations in the ECMWF velocity field and calculated the fractal dimension of the interface in figure 6 on different days. He found that, statistically, pair separations can be fitted equally well by linear as by exponential (Lyapunov) growth functions, and that the fractal dimension D (Wonhas & Vassilicos 2002*b*) of the interface in figure 6 is equal to 1 for the first three days but then increases above 1 until it reaches 1.48 on the last day of the simulation (day 15). Wonhas & Vassilicos (2002*b*) used these values of D with mixing law (3.4), where c'^2 is replaced by the total amount of ClONO₂, and

obtained diffusivity scalings $\kappa_t^{1-D/2}$ that agree with those found by Tan *et al.* (1998) for days beyond day 3. The different diffusivity scalings for different days correspond to different values of the time-dependent fractal dimension D .

It might be reasonable to expect the fractal dimension D to eventually converge to the space-filling value of 2 and pair separations to eventually grow exponentially (though, it must be said, Oseledec's (1968) theorem does *not* state that $h(\mathbf{x}, t)$ must necessarily tend to a *non-zero* asymptotic value, a common misconception in the literature). However, this chaotic behaviour does not appear to significantly influence mixing for a time as long as half a month in the simulations of Tan *et al.* (1998) and Wonhas & Vassilicos (2002*b*). The gradual appearance of global chaos might, however, explain the time growth of D , presumably towards the space-filling value of 2 that characterizes global chaotic advection. Nevertheless, the non-integral value of D might also reflect the spiral structure of the chemical concentration fields (figure 6).

This appears to be a case where the time T_{conv} required for the symptoms of global chaos to become detectable, i.e. well-defined Lyapunov exponents (even if finite-time ones) and space-filling interfacial structure (i.e. $D = 2$), is at least of the order of a month and therefore large enough for a lot of mixing and chemical reaction to occur by transient non-chaotic processes such as fractal/spiral mixing.

5. Stirring and mixing by turbulent flow

The idea that mixing as measured by the concentration variance is determined by the statistics of how fluid-element pairs are brought together by stirring (Durbin 1980; Falkovich *et al.* 2001) is valid quite generally, including turbulent flows. However, the explicit relation (3.3) between the concentration variance and pair separations has been derived under the assumption that concentration fluctuations occur over length-scales much smaller than those characterizing the flow, an assumption not valid in turbulent flows (except below the smallest (viscosity dominated) length-scale of the turbulence).

In the specific context of the classical phenomenology concerning statistically homogeneous, isotropic and non-decaying turbulent velocity fields (see Monin & Yaglom 1975), Thomson (1996) derived an explicit relation between the decay of the concentration variance and the average square pair separation, $\langle |\Delta|^2 \rangle (d/dt) c'^2 = -\frac{3}{2} c'^2 (d/dt) \langle |\Delta|^2 \rangle$. As in the case of equation (3.3), this relation applies when no source of scalar fluctuations is used to replenish the variance lost by mixing. From Richardson's law it then follows that c'^2 decays like $t^{-9/2}$ (Nelkin & Kerr 1981). This mixing law is different from the algebraic decay (3.4) that originates in the fractal/spiral mixing mechanism and also from the superexponential followed by exponential decay characteristic of globally chaotic mixing.

An understanding of turbulent mixing must start with some understanding of turbulent stirring and therefore of the mechanisms by which turbulence causes fluid-element pairs to move apart. According to Richardson (see Monin & Yaglom 1975) the eddies that are most effective in separating fluid elements are those that have a size comparable with the instantaneous separation between the two fluid elements. This idea is part and parcel of the classical phenomenology of turbulence (Monin & Yaglom 1975) which leads to Kolmogorov's $k^{-5/3}$ energy spectrum, Richardson's t^3 law and the $t^{-9/2}$ mixing law. To model the Richardson pair-separation mechanism requires a velocity difference and a decorrelation time for every separation spanning

the entire range of eddy scales. These velocity and time-scales can be derived from the energy spectrum of the turbulence.

Lagrangian stochastic models of turbulent-pair dispersion have been developed using continuous Markov processes and the entire range of velocity and time-scales just mentioned (Thomson 1990; Hoppe 1998). By their very nature, these models cannot take into account the topology of the velocity field, such as figure 5. Does this topology have an effect on turbulent pair dispersion?

Fluid-element accelerations are given by $D\mathbf{u}/Dt = \mathbf{a}$, and the topology of the velocity field is to a large extent determined by the incompressibility of the velocity field \mathbf{u} . This incompressibility operating on the previous equation implies

$$\nabla \cdot \mathbf{a} = \mathbf{s}^2 - \frac{1}{2}\boldsymbol{\omega}^2, \quad (5.1)$$

where \mathbf{s} is the strain matrix and $\boldsymbol{\omega}$ is the vorticity vector. Hence, $\nabla \cdot \mathbf{a}$ is large and positive most often in straining regions around hyperbolic points of the flow where \mathbf{s}^2 is large and $\boldsymbol{\omega}^2$ close to zero. Close fluid-element pairs can separate significantly where and when their accelerations strongly diverge, i.e. where and when $\nabla \cdot \mathbf{a}$ is large and positive. Provided the streamline structure of the turbulence is persistent enough in time, such separation events will therefore most often occur where close fluid-element pairs meet hyperbolic points. Straining regions surrounding hyperbolic points take pride of place in the cat-eye streamline structure of figures 3*a* and 5. As previously conjectured by Fung *et al.* (1992), provided streamline structures in the turbulence have some persistence, fluid-element pairs travel close to each other without separating significantly until they hit a straining region around a hyperbolic point and then separate violently. Some computational support for this view has been obtained by Fung & Vassilicos (1998) in their kinematic simulation of the turbulent flow of Paret & Tabeling (1997). Kinematic simulations are models of turbulent dispersion that do not use continuous Markov processes but, instead, use numerically constructed incompressible velocity fields with a manageable number of modes and a specified energy spectrum (see Fung *et al.* 1992). These simulations are inherently non-Markovian (in the sense that no delta correlation in time is used or assumed), and, if the energy spectrum they are given has a shape characteristic of turbulent flow, they incorporate all the velocity and time-scales required in Richardson's picture of pair separation. What they also incorporate, that Lagrangian stochastic models do not, is a flow topology, simply by virtue of being given a velocity field. This velocity field is essential for modelling the effect of straining regions on turbulent pair dispersion. The laboratory observations of Jullien *et al.* (1999) confirm that fluid-element pairs travel close to each other for a long time until they separate quite violently. This behaviour is in agreement with the very large flatness factors of their relative velocities found in turbulence (Yeung 1994). These large flatness factors are reproduced by kinematic simulation (Malik & Vassilicos 1999) but not by Lagrangian stochastic modelling, which under-predicts them by up to one order of magnitude (Hoppe 1998).

Fung & Vassilicos (1998) confirmed that kinematic simulation reproduces Richardson's law. A link between Richardson's law and the self-similar cat-eye streamline topology of figure 5 has been proposed by Davila & Vassilicos (2002) in terms of the fractal dimension D_s of the spatial distribution of straining hyperbolic points in the two-dimensional turbulence. By varying the power p of the energy spectrum

$E(k) \sim k^{-p}$ in their kinematic simulation they find that

$$\langle |\Delta|^2 \rangle \propto t^{4/D_s} \quad (5.2)$$

and that the value of D_s corresponding to the Kolmogorov spectrum $k^{-5/3}$ is $4/3$ (in three dimensions they find a power law t^{6/D_s} and $D_s = 2$ when $p = 5/3$).

6. Summary

Exponential pair separation is not pervasive in spatially smooth time-dependent flows. Lyapunov exponents might appear at asymptotically long times, but this asymptotic behaviour can occur after a long time, T_{conv} , in a majority of the flow and therefore be of restricted relevance to mixing. In the case of the stratospheric polar vortex, the spiral structure in figure 6 is transient, but what might be its effects on mixing and rates of chemistry last for at least half a month, if not more. Asymptotic behaviour should not detract from the potential importance of transient mechanisms when this transience is long lived.

Concentration variance measures mixing and is determined by fluid-element pair statistics. When global chaotic behaviour sets in quickly, exponential pair separation leads to superexponential variance decay in the short term. In the longer term, variance decay is exponential.

In steady and weakly unsteady two-dimensional vortices it is the spatial decorrelation of the concentration field produced by the field's spiral structure and measured by the fractal dimension D that causes accelerated mixing. Albeit accelerated, this decay of the concentration variance is only algebraic in time. Such a mixing mechanism occurs wherever spiral or fractal structures that are not space filling exist.

In turbulent flows, fluid-element pairs separate according to Richardson's law. Recent laboratory and computational research is showing that fluid-element pairs travel close to each other for a long time, until they separate quite suddenly. There are arguments and evidence to suggest that straining regions around hyperbolic points play an important role in the violent separation events, and that the self-similar topology of the hyperbolic points' spatial distribution (in the form of cat eyes within cat eyes in two dimensions) is closely related to Richardson's power law.

References

- Angilella, J. R. & Vassilicos, J. C. 1998 Spectral, diffusive and convective properties of fractal and spiral fields. *Physica D* **124**, 23–57.
- Antonsen, T. M., Fan, Z., Ott, E. & Garcia-Lopez, E. 1996 The role of chaotic orbits in the determination of power spectra of passive scalars. *Phys. Fluids* **8**, 3094–3104.
- Aref, H. 1984 Stirring by chaotic advection. *J. Fluid Mech.* **143**, 1–21.
- Batchelor, G. K. 1969 *An introduction to fluid dynamics*. Cambridge University Press.
- Chipperfield, M. P., Lutman, E. R., Kettleborough, J. A. & Pyle, J. A. 1997 Model studies of chlorine deactivation and formation of ClONO₂ collar in the arctic polar vortex. *J. Geophys. Res.* **102**, 1467–1478.
- Davila, J. & Vassilicos, J. C. 2002 Richardson pair diffusion and the stagnation point structure of turbulence. *Phys. Rev. Lett.* Preprint. (Available from <http://arxiv.org/abs/physics/0207108>.)
- Durbin, P. A. 1980 A stochastic model of two-particle dispersion and concentration fluctuations in homogeneous turbulence. *J. Fluid Mech.* **100**, 279–302.

- Eckhardt, B. & Yao, D. 1993 Local Lyapunov exponents in chaotic systems. *Physica D* **65**, 100–108.
- Eckmann, J. P. & Ruelle, D. 1985 Ergodic theory of chaos and strange attractors. *Rev. Mod. Phys.* **57**, 617–656.
- Falkovich, G., Gawedzki, K. & Vergassola, M. 2001 Particles and fields in fluid turbulence. *Rev. Mod. Phys.* **73**, 913–975.
- Fereday, D., Haynes, P., Wonhas, A. & Vassilicos, J. C. 2002 Scalar variance decay in chaotic advection and Batchelor-regime turbulence. *Phys. Rev. E* **65**, 353011–353014.
- Flohr, P. & Vassilicos, J. C. 1997 Accelerated scalar dissipation in a vortex. *J. Fluid Mech.* **348**, 295–317.
- Fung, J. C. H. & Vassilicos, J. C. 1991 Fractal dimensions of lines in chaotic advection. *Phys. Fluids A* **11**, 2725–2733.
- Fung, J. C. H. & Vassilicos, J. C. 1998 Two-particle dispersion in turbulentlike flows. *Phys. Rev. E* **57**, 1677–1690.
- Fung, J. C. H., Hunt, J. C. R., Malik, N. A. & Perkins, R. J. 1992 Kinematic simulation of homogeneous turbulent flows generated by unsteady random Fourier modes. *J. Fluid Mech.* **236**, 281–318.
- Hepe, B. M. O. 1998 Generalized Langevin equation for relative turbulent dispersion. *J. Fluid Mech.* **357**, 167–198.
- Jullien, M.-C., Paret, J. & Tabeling, P. 1999 Richardson pair diffusion in two-dimensional turbulence. *Phys. Rev. Lett.* **82**, 2872–2875.
- Lichtenberg, A. J. & Leiberman, M. A. 1983 *Regular and stochastic motion*. Springer.
- McIntyre, M. E. 1995 The stratospheric polar vortex and sub-vortex: fluid dynamics and mid-latitude ozone loss. *Phil. Trans. R. Soc. Lond. A* **352**, 227–240.
- Malik, N. A. & Vassilicos, J. C. 1999 A Lagrangian model of turbulent dispersion with turbulent-like flow structure: comparison with direct numerical simulation for two-particle statistics. *Phys. Fluids* **11**, 1572–1580.
- Monin, A. S. & Yaglom, A. M. 1975 *Statistical fluid dynamics*, vol. 2. Boston, MA: MIT Press.
- Nelkin, M. & Kerr, R. M. 1981 Decay of scalar variance in terms of a modified Richardson law for pair dispersion. *Phys. Fluids* **24**, 1754–1756.
- Oseledec, V. I. 1968 A multiplicative ergodic theorem: Lyapunov characteristic numbers for dynamical systems. *Trans. Moscow Math. Soc.* **19**, 197–231.
- Ott, E. & Antonsen, T. M. 1989 Fractal measures of passively convected vector field and scalar gradients in chaotic flows. *Phys. Rev. A* **39**, 3660–3671.
- Ottino, J. 1989 *The kinematics of mixing: stretching, chaos, and transport*. Cambridge University Press.
- Paret, J. & Tabeling, P. 1997 Experimental observation of the two-dimensional inverse energy cascade. *Phys. Rev. Lett.* **79**, 4162–4165.
- Peter, T. 1994 The stratospheric ozone layer: an overview. *Environ. Pollut.* **83**, 69–79.
- Pierrehumbert, R. T. 1994 Tracer microstructure in the large-eddy dominated regime. *Chaos Solitons Fractals* **4**, 1111–1116.
- Pyle, J. A. 1995 Ozone loss in middle latitudes and the role of the Arctic polar vortex. *Phil. Trans. R. Soc. Lond. A* **352**, 241–245.
- Tan, D. G. H., Haynes, P. H., MacKenzie, A. R. & Pyle, J. A. 1998 Effects of fluid dynamical stirring and mixing on the deactivation of stratospheric chlorine. *J. Geophys. Res.* **103**, 1585–1605.
- Thomson, D. J. 1990 A stochastic model for the motion of particle pairs in isotropic high-Reynolds number turbulence, and its application to the problem of concentration variance. *J. Fluid Mech.* **210**, 113–153.
- Thomson, D. J. 1996 The second-order moment structure of dispersing plumes and puffs. *J. Fluid Mech.* **320**, 305–329.

- Toussaint, V. & Carrière, P. 1999 Diffusive cut-off scale of fractal surfaces in chaotic mixing. *Int. J. Bifurcat. Chaos* **9**, 443–454.
- Toussaint, V., Carrière, P. & Raynal, F. 1995 A numerical Eulerian approach to mixing by chaotic advection. *Phys. Fluids* **7**, 2587–2600.
- Vassilicos, J. C. & Hunt, J. C. R. 1991 Fractal dimensions and spectra of interfaces with application to turbulence. *Proc. R. Soc. Lond. A* **435**, 505–534.
- Wonhas, A. 2001 Mixing and geometry of scalar fields in vortical and chaotic flows. PhD thesis, University of Cambridge, UK.
- Wonhas, A. & Vassilicos, J. C. 2001 Mixing in frozen and time-periodic two-dimensional vortical flows. *J. Fluid Mech.* **442**, 359–385.
- Wonhas, A. & Vassilicos, J. C. 2002a Mixing in fully chaotic flows. *Phys. Rev. E*. (In the press.)
- Wonhas, A. & Vassilicos, J. C. 2002b Diffusivity dependence of ozone depletion over the mid-northern latitudes. *Phys. Rev. E* **65**, 051111.
- Yeung, P. K. 1994 Direct numerical simulation of two-particle relative diffusion in isotropic turbulence. *Phys. Fluids* **6**, 3416–3428.

AUTHOR PROFILE

J. C. Vassilicos

Born in Athens, Greece, Christos Vassilicos studied physics in Brussels and did his doctoral research at the Department of Applied Mathematics and Theoretical Physics of the University of Cambridge. He obtained his PhD in 1990 and was awarded a Royal Society University Research Fellowship in 1994, which he will hold until 2004. He joined Imperial College as Reader in Fluid Mechanics in January 2001.

